Communications in Physics, Vol. 34, No. 3 (2024), pp. 249-258
DOI: https://doi.org/10.15625/0868-3166/21022

Multiple mobility edges in quasi-periodic mosaic lattices revisited: A numerical study based on time-dependent reflection

Ba Phi Nguyen[1,2,†]

[1]*Department of Basic Sciences, Mientrung University of Civil Engineering, Tuy Hoa 620000, Vietnam*

[2]*Mathematics and Physics Research Group, Mientrung University of Civil Engineering, Tuy Hoa 620000, Vietnam*

E-mail: [†]nguyenbaphi@muce.edu.vn

Received 25 June 2024

Accepted for publication 26 August 2024

Published 5 September 2024

Abstract. *The dynamics of a short wave packet in one-dimensional quasi-periodic lattices with mosaic modulated on-site potentials is investigated numerically. This model is characterized by the modulation period κ and the quasi-periodic potential strength λ. For parabolic wave packets with a given central energy E_0, we calculate the averaged time-dependent reflectance, $\langle R(t)\rangle$, for various values of κ and λ. From the extensive numerical calculations, we show that there exist multiple mobility edges in such a model with the number of mobility edges to be always equal to $2(\kappa-1)$.*

Keywords: Quasi-periodic mosaic lattices; Anderson localization; mobility edges; time-dependent reflection.

Classification numbers: 72.15.Rn; 71.23.An; 72.20.Ee; 73.23.-b; 03.65.Ta.

1. Introduction

The study of the transport and localization properties of non-interacting quantum particles in disordered systems is an old, yet all-important problem in various branches of physics. One of the most fundamental phenomena in such systems is localization that was first predicted by P. W. Anderson over 60 years ago [1]. This so-called Anderson localization is well-known as a consequence of the quantum interference effect of a scattered wave function in disordered media [2–4].

According to the prediction of the scaling theory of localization [5], wave-like excitations in one-dimensional (1D) and two-dimensional (2D) disordered systems are always localized exponentially in the presence of an arbitrarily weak disorder, whereas a phase transition from extended to localized states is expected to take place in three-dimensional (3D) case when the disorder strength is beyond a certain critical value.

In spite of being an important element in leading to Anderson localization, the random disorder is not a prerequisite for occurring localization. Indeed, there exists a family of systems, the so-called quasi-periodic systems, in which potential is aperiodic but deterministic [6,7]. Unlike disordered systems for which the metal-insulator transition may only occur in three dimensions [8,9], quasi-periodic systems can exhibit a phase transition in one [10–13], quasi-one [14, 15] and two dimensions [16, 17]. In recent years, quasi-periodic systems have become one of the most promising candidates to study quantum localization both theoretically and experimentally. This arises from the fact that they are much easier to implement than those with random disorders. One of the simplest but most famous members of the quasi-periodic family is the Aubry-André-Harper (AAH) model [7], which exhibits a global phase transition from extended to localized states at a critical value of the quasi-periodic potential strength. The energy-dependent mobility edge, which corresponds to critical energy separating extended and localized states, has been proven to be absent in the AAH model [8, 18]. Nowadays, however, it is well-known that by breaking energy-independent duality symmetry at the transition point, such mobility edges were predicted to exist in some generalized AAH models as well as in other quasi-periodic ones [19–21]. Some recent experimental observations have confirmed the theoretical prediction [13, 22].

In the context of quasi-periodic systems, a class of exactly solvable 1D models has been recently proposed by Wang and co-workers [23]. This so-called quasi-periodic mosaic model is characterized by a positive integer number κ, the so-called inlay parameter. In the case of $\kappa = 1$, the quasi-periodic mosaic model reduces to the familiar AAH model. By varying the inlay parameter κ ($\kappa \neq 1$), the authors have shown analytically and numerically the existence of multiple mobility edges in this kind of model. Inspired by this work, there are some novelty and interesting findings that have been shown in recent studies [24–27] for which the related aspects of the mosaic lattice model have been considered. One of the most typical examples was demonstrated in Ref. [24], where Zeng and co-workers [24] added a term of p-wave superconducting pairing into the original quasi-periodic mosaic model [23]. Based on calculating energy spectra and topological invariant of the system, it has been found that the interplay between mosaic modulation in the on-site potentials and superconducting pairing may give rise to the existence of Majorana zero modes, which play an important role in implementing topological quantum computation [28]. In another example, when the mosaic modulation in the on-site potentials is replaced by the mosaic modulation in the hopping amplitudes, the obtained model is called a quasi-periodic off-diagonal mosaic lattice one [26]. In the case of the mosaic lattice being commensurate, it has been shown that topological edge modes with zero and non-zero energies can exist by tuning the mosaic modulations. Meanwhile, if the mosaic lattice becomes incommensurate, the Anderson localization will show up.

The main aim of the present paper is to verify some behaviors presented in a recent work [23] by using a formalism based on time-dependent reflection proposed in Ref. [29]. The numerical experimental results indicate that the mosaic modulation in the on-site potentials significantly

alters localization properties. In particular, a delocalization-localization transition is found to occur at the quasi-periodic potential strength in the present model to be smaller than that in the AAH model. In addition, the number of mobility edges in the 1D quasi-periodic mosaic systems is always equal to $2(\kappa-1)$. These findings are consistent with those presented in Ref. [23]. Note that the reflection geometry formalism has also been employed recently by us in investigating the time evolution of wave packets incident on a disordered mosaic lattice chain [30].

The rest of this paper is organized as follows. In Sec. 2, we present the 1D quasi-periodic mosaic lattice model characterized by the time-independent Schrödinger equation within the nearest-neighbor tight-binding approximation. In addition, the numerical calculation method, as well as the physical quantities of interest, are described briefly in this section. In Sec. 3, we present our numerical results and discussions. Finally, in Sec. 4, we conclude the paper.

2. Theoretical model and formalism

2.1. Model

We consider a 1D tight-binding lattice model within nearest-neighbor approximation which is described by a discrete stationary Schrödinger equation

$$J(\psi_{n-1}+\psi_{n+1})+\varepsilon_n\psi_n = E\psi_n, \tag{1}$$

where ψ_n and ε_n are the wave function amplitude and the on-site potential at the nth lattice site, respectively. E is the energy and J is the coupling strength between nearest-neighbor sites. From now on, we will measure all energy scaled in units of J and set it equal to 1. In this study, we will investigate the transport and localization properties of a model, which is the so-called quasi-periodic mosaic lattice model [23]. This model is defined by

$$\varepsilon_n = \begin{cases} 2\lambda\cos(2\pi\gamma n+\phi), & n = m\kappa, \\ 0, & \text{otherwise}, \end{cases} \tag{2}$$

where λ is the quasi-periodic potential strength and ϕ is a random phase uniformly distributed in an interval $[0,2\pi]$. γ is the spatial modulation frequency that is taken as the inverse of the golden mean, $\gamma=(\sqrt{5}-1)/2$ [31]. The inlay parameter κ representing the period of the mosaic modulation is a fixed positive integer larger than 1 and m is an integer running from 1 to N. Then the total number of sites L is equal to κN. As mentioned above, the present model reduces to the famous AAH model in the case of $\kappa=1$. This model exhibits a transition from completely extended states for $\lambda<1$ to completely localized ones for $\lambda>1$ without generating a mobility edge. To address the question of how this changes for $\kappa\neq 1$, Wang and co-workers have shown that the Anderson transition still occurs in this situation [23]. More interestingly, they have demonstrated analytically and numerically that there exist $2(\kappa-1)$ mobility edges which are distributed symmetrically in energy spectra.

2.2. Method

We assume that a wave packet is incident from the left side of the quasi-periodic region under consideration. Then the amplitudes of the incident, reflected, and transmitted waves, A, B, and C are defined by

$$\psi_n = \begin{cases} Ae^{iqn}+Be^{-iqn}, & n\leq 2, \\ Ce^{iqn}, & n\geq L-1, \end{cases} \tag{3}$$

where the wave number q is related to E by the free-space dispersion relationship $E = 2\cos q$. In the absence of dissipation, the law of energy conservation $|B|^2 + |C|^2 = |A|^2$ should be satisfied.

In order to solve Eq. (1) numerically, we first fix ψ_{L-1} to 1, then we obtain $C = \exp[-iq(L-1)]$ and $\psi_L = \exp(iq)$. Knowing the values of ψ_L and ψ_{L-1}, we can solve Eq. (1) iteratively to obtain ψ_{L-2}, $\psi_{L-3}, \ldots,$ ψ_1. Using the definition of A and B given in Eq. (3), we can express them in terms of ψ_1 and ψ_2:

$$A = e^{-2iq}\frac{\psi_2 - \psi_1 e^{-iq}}{1 - e^{-2iq}},\ B = \frac{\psi_1 e^{iq} - \psi_2}{1 - e^{-2iq}}. \tag{4}$$

In this study, we focus on the behavior of the reflection coefficient $\tilde{r}(E)$ and the reflectance $\tilde{R}(E)$ defined by

$$\tilde{r}(E) = \frac{B}{A} = e^{2iq}\frac{\psi_1 e^{iq} - \psi_2}{\psi_2 - \psi_1 e^{-iq}}, \tag{5}$$

$$\tilde{R}(E) = \left|\frac{B}{A}\right|^2 = \left|\frac{\psi_1 e^{iq} - \psi_2}{\psi_2 - \psi_1 e^{-iq}}\right|^2. \tag{6}$$

In the time-domain, the time-dependent reflection coefficient $r(t)$ and the disorder-averaged time-dependent reflectance $\langle R(t)\rangle$ are given by [29, 30]

$$r(t) = \frac{1}{2\pi}\int_{-2}^{2} dE\tilde{r}(E)\tilde{f}(E)\exp(iEt), \tag{7}$$

$$\langle R(t)\rangle = \langle |r(t)|^2\rangle = \frac{1}{(2\pi)^2}\int_{-2}^{2} dE_1 \int_{-2}^{2} dE_2 \langle \tilde{r}(E_1)\tilde{r}^*(E_2)\rangle \tilde{f}(E_1)\tilde{f}^*(E_2)\exp[i(E_1 - E_2)t]. \tag{8}$$

It is worth noting here that due to $r(t)$ and $\langle R(t)\rangle$ being defined through the amplitudes of the incident and reflected waves which exist only outside the disordered region, the integrations (7) and (8) are restricted in the energy interval $[-2, 2]$. To study the time dependence of $r(t)$ and $\langle R(t)\rangle$, we consider a parabolic wave packet characterized by the spectrum

$$\tilde{f}(E) = \sqrt{\frac{15\pi}{16\sigma}}\left[1 - \frac{(E - E_0)^2}{4\sigma^2}\right], |E - E_0| < 2\sigma. \tag{9}$$

Here E_0 and σ are the central energy and the spectral width of the incident wave packet, respectively. Following the existing theories of localization in the time domain, [32–35], global characterization of the diffusion and localization properties of a wave packet is provided by the time evolution of the reflectance. Specifically, a power-law decay in the long-time limit is expected for the averaged time-dependent reflectance: $\langle R(t)\rangle$ should decrease as t^{-2} in the localized regime and as $t^{-3/2}$ in the diffuse regime. It is worth noting that studying the energy-dependent mobility edge based on the measurements in the reflection geometry has substantial experimental advantages over more conventional approaches in the transmission geometry, in that the reflectance is often more easily measurable than the transmittance, and there exist situations where measurements in the transmission mode are not possible. These advantages are especially relevant to fields such as optics and acoustics. Theoretically, the formalism employed in the present work consumes less computational resources than the conventional method of matrix diagonalization used in Ref. [23], especially for large-sized systems.

3. Computational results

In our calculations, we have calculated $\langle R(t)\rangle$ by averaging over 10000 different configurations of ε_n. The step size in energy ΔE and the system size L are fixed to be 10^{-3} and 1000, respectively. Besides, we consider parabolic wave packets with a fixed spectral width of $\sigma = 0.05$. Note that the time t should be scaled by $\hbar/J$.

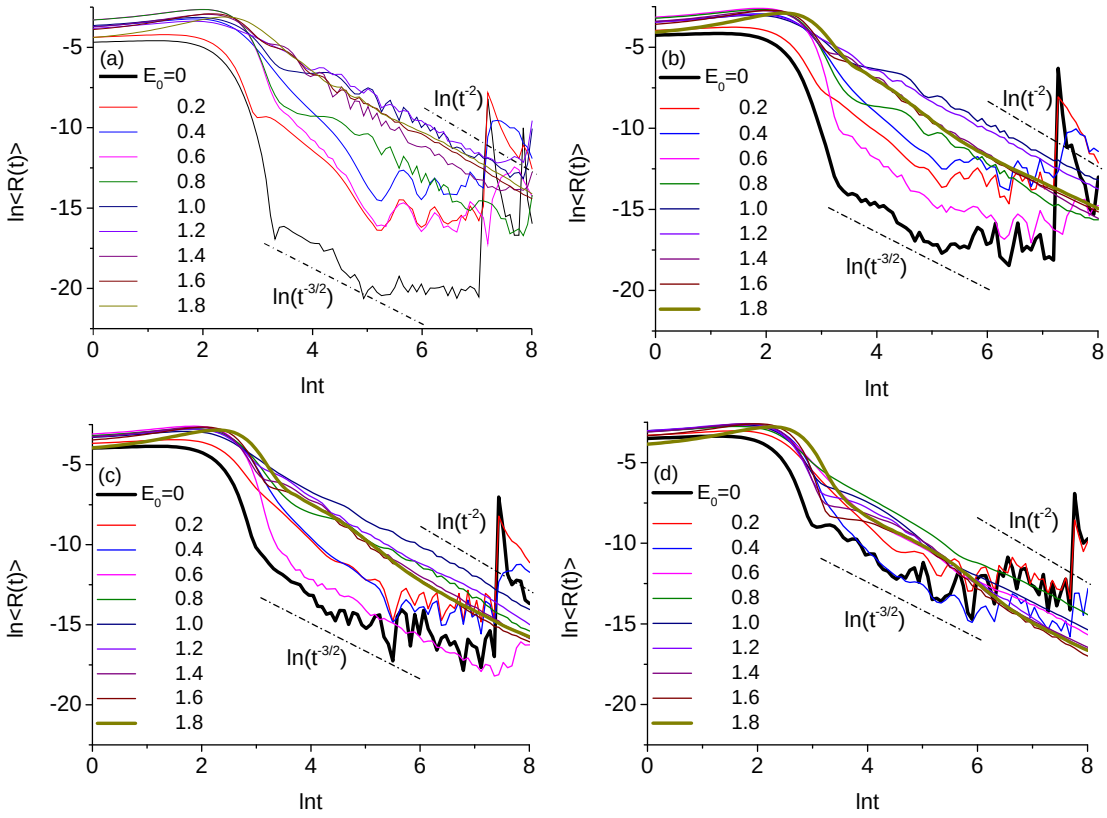

Fig. 1. ln–ln plot of the disorder-averaged time-dependent reflectance $\langle R(t)\rangle$ versus time t when $\kappa = 2$ for (a) $\lambda = 0.75$, (b) $\lambda = 1.0$, (c) $\lambda = 1.25$, and (d) $\lambda = 2.0$. Different curves correspond to values of the central energy E_0 of the incident wave packet. It is shown that for incident wave packets with E_0 near the band edges (e.g., $E_0 = 1.8$, the bold dark yellow curve), $\langle R(t)\rangle \propto t^{-2}$ in the long-time limit.

In Fig. 1, we plot the time evolution of $\langle R(t)\rangle$ for various values of the central energy E_0 of the incident wave packet when (a) $\lambda = 0.75$, (b) $\lambda = 1.0$, (c) $\lambda = 1.25$, and (d) $\lambda = 2.0$ in the case of $\kappa = 2$. Based on the existing theories of localization in the time domain [32–35], one predicts that the time evolution of $\langle R(t)\rangle$ obeys a power law as $\langle R(t)\rangle \propto t^{-\alpha}$ in the long-time limit. In particular, for incident wave packets with E_0 near the band edges ($E = \pm 2$), we observe that $\langle R(t)\rangle$ decays according to a power law with an exponent α very close to 2. This indicates the behavior of Anderson localization for such incident wave packets. Moreover, this behavior takes

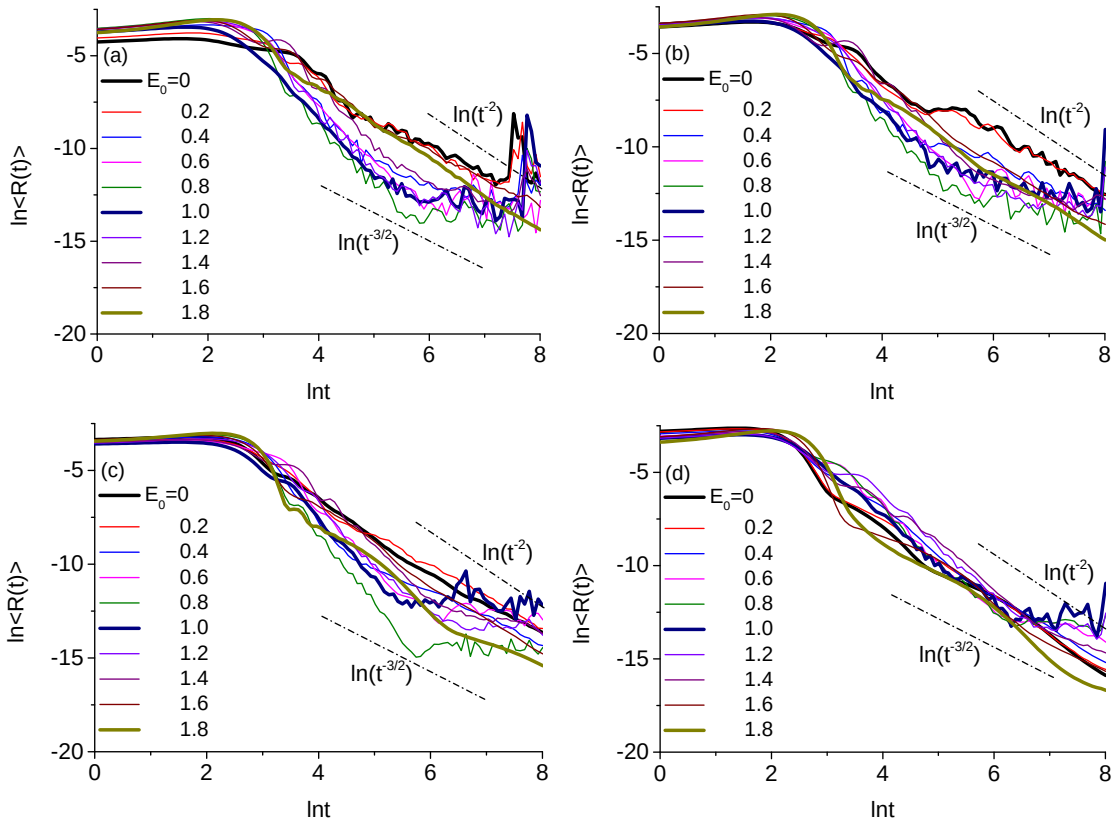

Fig. 2. ln–ln plot of the disorder-averaged time-dependent reflectance $\langle R(t)\rangle$ versus time t when $\kappa = 3$ for (a) $\lambda = 0.75$, (b) $\lambda = 1.0$, (c) $\lambda = 1.25$, and (d) $\lambda = 2.0$. When $\lambda > 1$ we find that there exist two localized energy ranges around the band center (the bold black curve) and near the band edge (the bold dark yellow curve), and one diffusive energy range between them (e.g., $E_0 = 1.0$, the bold navy curve).

place even in the case of $\lambda < 1$ [see Fig. 1(a)]. This means that the critical value of λ for the occurring Anderson transition in the quasi-periodic mosaic model is smaller than that in the AAH model. Remarkably, there appears an energy range E_0 around the band center ($E = 0$) in which incident wave packets exhibit deviation from the Anderson localization behavior (i.e., $\alpha \neq 2$). The width of this energy range will narrow down gradually with increasing λ [e.g., $E_0 \in (-1, 1)$ and $(-0.8, 0.8)$ corresponding to the cases of $\lambda = 1.0$ and 1.25] and reach a saturation width at a certain critical value of λ [$E_0 \in (-0.6, 0.6)$ at $\lambda \simeq 2$]. Within such energy intervals, although $\langle R(t)\rangle$ shows oscillations with time, its decay can be approximately described by the law $\langle R(t)\rangle \propto t^{-3/2}$ for an intermediate time. This is considered to be a hallmark of diffusion behavior. In the diffuse regime, the reflection of the coherent part of the wave packet from the other end of the system starts to become visible in the reflected signal which produces peaks in $\langle R(t)\rangle$ in the long-time limit (see the bold black curve, for example). Note that we have already plotted both $\langle R(t)\rangle$ versus time t and ln-ln plot of $\langle R(t)\rangle$ versus time t. It has been shown that the peaks in $\langle R(t)\rangle$ appear in these

two forms. In short, if one considers incident wave packets with $E_0 \in [0,2]$, there exists a critical value of E_0 above (below) which incident wave packet exhibits localized (diffuse) behavior. The value of critical energy depends on the strength of on-site potential λ in the quasi-periodic mosaic lattice. The set of all obtained values of critical energy when we change λ gives rise to a mobility edge which seperates localization and diffusive phases. Similar findings are also obtained for incident wave packets with $E_0 \in [-2,0]$. This implies that there exist two mobility edges in the whole energy band in the case of $\kappa = 2$.

Similarly, in Fig. 2, we depict the time evolution of $\langle R(t)\rangle$ for different values of E_0 and λ when $\kappa = 3$. It is found that when $\lambda < 1$ [see Fig. 2(a)], almost all incident wave packets are diffuse except for incident wave packets with E_0 near the band edges which show the localization behavior, $\langle R(t)\rangle \propto t^{-2}$. However, when $\lambda > 1$ [see Figs. 2(b)-(d)] we find that there exist two energy ranges around the central values of $E_0 = 0$ and $E_0 = 1.8$ indicating the localization behavior, one energy range around the central value of $E_0 = 1.0$ indicating the diffusive behavior. This implies that there are four mobility edges in the quasi-periodic mosaic lattice model with $\kappa = 3$. The appearance of alternating diffusive and localized energy intervals in the whole energy band is also shown to exist for the larger values of κ. The number of such energy intervals, hence mobility edges increases with increasing κ. This argument is supported by the numerical data shown in Fig. 3. Accordingly, there present two diffusive energy ranges around the central values of $E_0 = 0$ and $E_0 = 1.4$ for which $\langle R(t)\rangle \propto t^{-3/2}$, and one localized energy range between them for which $\langle R(t)\rangle \propto t^{-2}$. This means that there are six mobility edges in the case of $\kappa = 4$.

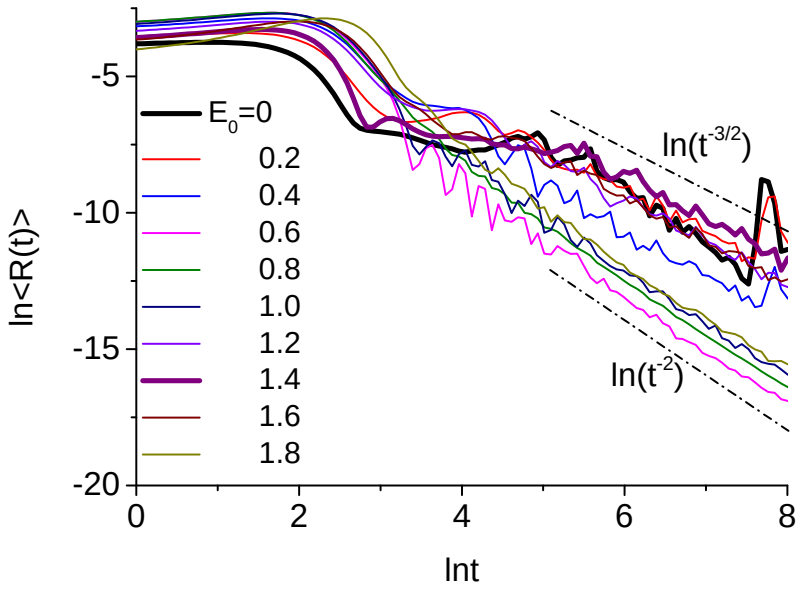

Fig. 3. ln–ln plot of the disorder-averaged time-dependent reflectance $\langle R(t)\rangle$ versus time t when $\kappa = 4$ and $\lambda = 2.0$ for different values of E_0. The appearance of alternating diffusive and localized energy intervals is observed clearly in this case.

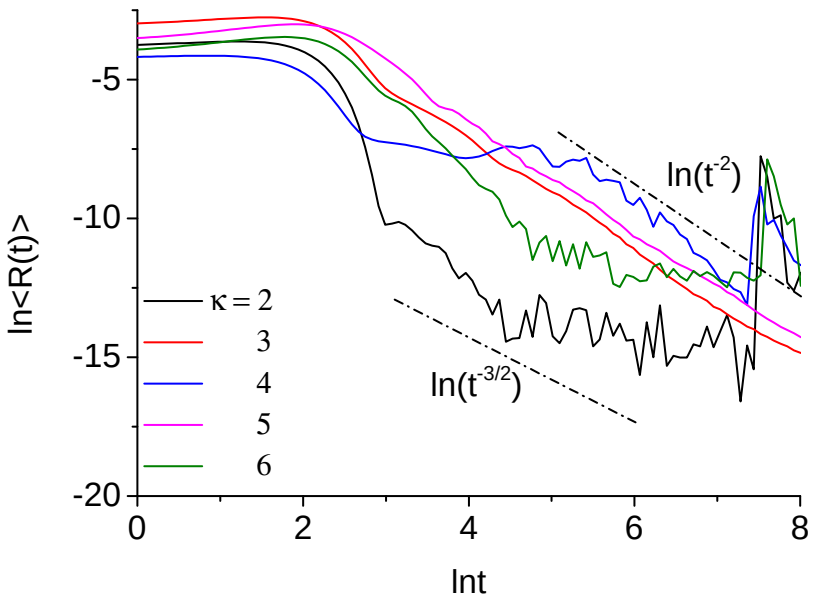

Fig. 4. ln–ln plot of the disorder-averaged time-dependent reflectance $\langle R(t)\rangle$ versus time t when $E_0 = 0$ and $\lambda = 2.0$ for different values of κ. The cases of $\kappa = 2,\ 4$ and 6 indicate the diffusive behavior, whereas the ones of $\kappa = 3$ and 5 show the localization one.

Based on the results presented in Figs. 1, 2 and 3, we conclude that the inlay parameter κ alters significantly diffusive and localized properties. The presence of the mosaic modulations in the on-site potentials is shown to be able to give rise to the existence of multiple mobility edges in the 1D quasi-periodic lattice. In particular, the number of mobility edges is found to be always equal to $2(\kappa - 1)$ in the system under consideration. This was first pointed out by Wang and co-works when they considered the same problem but with the alternative formalism [23]. Before closing the present study, we pay special attention to the case of $E_0 = 0$. In Fig. 4, we present the time evolution of $\langle R(t)\rangle$ at $E_0 = 0$ when $\lambda = 2.0$ for different values of κ. Interestingly, it is found that the incident wave packet with $E_0 = 0$ traveling in a quasi-periodic mosaic system with even κ will always be diffusive while those with odd κ will become localized when the strength of the quasi-periodic potential becomes sufficiently strong ($\lambda > 1$).

4. Conclusions

In this paper, we have numerically investigated the diffusion and localization properties of a wave packet in the 1D mosaic lattice whose quasi-periodic on-site potentials are modulated for equally spaced sites. Using the formalism proposed in Ref. [29], we have calculated and analyzed the time evolution of the reflectance. Based on the numerical results we find and confirm that the interval of the mosaic modulation (also known as the inlay parameter) κ alters diffusive and localization properties significantly. Like the AAH model, the Anderson transition is also found to take place in the quasi-periodic mosaic model but the critical value of the quasi-periodic potential strength is smaller than that in the AAH model. However, in contrast to the AAH model for which

no mobility edges exist, the appearance of multiple mobility edges has been found in the lattice model under consideration. The number of mobility edges is associated with the inlay parameter and equal to $2(\kappa - 1)$. In addition, an incident wave packet with the central energy around the center of the band will always be diffusive for even κ whereas it will become localized for odd κ in the case of quasi-periodic potential strength becomes sufficiently strong. All our results are consistent with the results presented by Wang and co-workers [23].

Acknowledgements

I would like to thank Prof. Kihong Kim for careful reading the manuscript and for giving useful comments.

References

[1] P. W. Anderson, *Absence of diffusion in certain random lattices*, Phys. Rev. **109** (1958) 1492.
[2] I. M. Lifshits, A. S. Gredeskul and L. A. Pastur, *Introduction to the theory of disordered systems*, Wiley-VCH, 1988.
[3] P. Sheng, *Introduction to wave scattering, localization, and mesoscopic phenomena*, vol. 88. Springer Berlin, Heidelberg, 2006.
[4] A. Lagendijk, B. A. van Tiggelen and D. Wiersma, *Fifty years of Anderson localization*, Phys. Today **62** (2009) 24.
[5] E. Abrahams, P. W. Anderson, D. C. Licciardello and T. V. Ramakrishnan, *Scaling Theory of Localization: Absence of Quantum Diffusion in Two Dimensions*, Phys. Rev. Lett. **42** (1979) 673.
[6] P. G. Harper, *Single Band Motion of Conduction Electrons in a Uniform Magnetic Field*, Proc. Phys. Soc. A **68** (1955) 874.
[7] S. Aubry and G. André, *Analyticity breaking and Anderson localization in incommensurate lattices*, Ann. Israel. Phys. Soc. **3** (1980) 133.
[8] P. A. Lee and T.V. Ramakrishnan, *Disordered electronic systems*, Rev. Mod. Phys. **57** (1985) 287.
[9] F. Evers and A. D. Mirlin, *Anderson transitions*, Rev. Mod. Phys. **80** (2008) 1355.
[10] G. Roati *et al.*, *Anderson localization of a non-interacting Bose–Einstein condensate*, Nature **453** (2008) 895.
[11] Y. Lahini *et al.*, *Observation of a Localization Transition in Quasiperiodic Photonic Lattices*, Phys. Rev. Lett. **103** (2009) 013901.
[12] J. Biddle, D. J. Priour, Jr. B. Wang and S. Das Sarma, *Localization in one-dimensional lattices with non-nearest-neighbor hopping: Generalized Anderson and Aubry-André models*, Phys. Rev. B **83** (2011) 075105.
[13] H. P. Lüschen *et al.*, *Single-Particle Mobility Edge in a One-Dimensional Quasiperiodic Optical Lattice*, Phys. Rev. Lett. **120** (2018) 160404.
[14] M. Rossignolo and L. Dell'Anna, *Localization transitions and mobility edges in coupled Aubry-André chains*, Phys. Rev. B **99** (2019) 054211.
[15] R. Wang, X. M. Yang and Z. Song, *Localization transitions and mobility edges in quasiperiodic ladder*, J. Phys.: Condens. Matter **33** (2021) 365403.
[16] A.-M. Guo, X. C. Xie and Q.-F. Sun, *Delocalization and scaling properties of low-dimensional quasiperiodic systems*, Phys. Rev. B **89** (2014) 075434.
[17] B. Huang and W. V. Liu, *Moiré localization in two-dimensional quasiperiodic systems*, Phys. Rev. B **100** (2019) 144202.
[18] N. F. Mott, *Metal–insulator transitions*, Phys. Today **31** (1978) 42.
[19] S. Das Sarma, A. Kobayashi and R. E. Prange, *Proposed Experimental Realization of Anderson Localization in Random and Incommensurate Artificially Layered Systems*, Phys. Rev. Lett. **56** (1986) 1280.
[20] J. Biddle and S. Das Sarma, *Predicted Mobility Edges in One-Dimensional Incommensurate Optical Lattices: An Exactly Solvable Model of Anderson Localization*, Phys. Rev. Lett. **104** (2010) 070601.
[21] A. Purkayastha, A. Dhar and M. Kulkarni, *Nonequilibrium phase diagram of a one-dimensional quasiperiodic system with a single-particle mobility edge*, Phys. Rev. B **96** (2017) 180204R.

[22] F. A. An, Eric J. Meier and B. Gadway, *Engineering a Flux-Dependent Mobility Edge in Disordered Zigzag Chains*, Phys. Rev. X **8** (2018) 031045.
[23] Y. Wang *et al.*, *One-Dimensional Quasiperiodic Mosaic Lattice with Exact Mobility Edges*, Phys. Rev. Lett. **125** (2020) 196604.
[24] Q.-B. Zeng, R. Lü and L. You, *Topological superconductors in one-dimensional mosaic lattices*, EPL **135** (2021) 17003.
[25] Y. Liu, Y. Wang, X.-J. Liu, Q. Zhou and S. Chen, *Exact mobility edges, PT-symmetry breaking, and skin effect in one-dimensional non-Hermitian quasicrystals*, Phys. Rev. B **103** (2021) 014203.
[26] Q.-B. Zeng and R. Lü, *Topological phases and Anderson localization in off-diagonal mosaic lattices*, Phys. Rev. B **104** (2021) 064203.
[27] L. Gong, *Exact mobility edges in one-dimensional mosaic lattices inlaid with slowly varying potentials*, Adv. Theory Simul. **4** (2021) 2100135.
[28] S. D. Sarma, M. Freedman and C. Nayak, *Majorana zero modes and topological quantum computation*, npj Quantum Inf. **1** (2015) 15001.
[29] S. E. Skipetrov and A. Sinha, *Time-dependent reflection at the localization transition*, Phys. Rev. B **97** (2018) 104202.
[30] B. P. Nguyen, D. K. Phung and K. Kim, *Quasiresonant diffusion of wave packets in one-dimensional disordered mosaic lattices*, Phys. Rev. B **106** (2022) 134204.
[31] X. Li, X. Li and S. Das Sarma, *Mobility edges in one-dimensional bichromatic incommensurate potentials*, Phys. Rev. B **96** (2017) 085119.
[32] B. White, P. Sheng, Z. Q. Zhang and G. Papanicolaou, *Wave localization characteristics in the time domain*, Phys. Rev. Lett. **59** (1987) 1918.
[33] M. Titov and C. W. J. Beenakker, *Signature of Wave Localization in the Time Dependence of a Reflected Pulse*, Phys. Rev. Lett. **85** (2000) 3388.
[34] S. E. Skipetrov and B. A. van Tiggelen, *Dynamics of weakly localized waves*, Phys. Rev. Lett. **92** (2004) 113901.
[35] S. E. Skipetrov and B. A. van Tiggelen, *Dynamics of Anderson localization in open 3D media*, Phys. Rev. Lett. **96** (2006) 043902.